INTERNATIONAL JOURNAL FOR NUMERICAL METHODS IN FLUIDS
Int. J. Numer. Meth. Fluids 2009; **59**:443–458
Published online 2 June 2008 in Wiley InterScience (www.interscience.wiley.com). DOI: 10.1002/fld.1825

Slip effects and heat transfer analysis in a viscous fluid over an oscillatory stretching surface

Z. Abbas[1,2,*,†], Y. Wang[1,3], T. Hayat[4] and M. Oberlack[1]

[1]*Chair of Fluid Dynamics, Department of Mechanical Engineering, Darmstadt University of Technology, Darmstadt 64289, Germany*
[2]*Department of Mathematics, Faculty of Basic and Applied Sciences, IIU, Islamabad 44000, Pakistan*
[3]*Institute of Geotechnical Engineering, University of Natural Resources and Applied Life Sciences, Feistmantelstrasse 4, 1180 Vienna, Austria*
[4]*Department of Mathematics, Quaid-I-Azam University 45320, Islamabad 44000, Pakistan*

SUMMARY

In this study, we investigate the heat transfer problem in a viscous fluid over an oscillatory infinite sheet with slip condition. The sheet is moved back and forth in its own plane. The derived problem involves a dimensionless parameter indicating the relative magnitude of frequency to sheet stretching rate. A system of non-linear partial differential equations is solved numerically using the finite-difference scheme, in which a coordinate transformation is employed to transform the semi-infinite physical space to a bounded computational domain. The physical features of interesting parameters on the velocity and temperature distributions are shown graphically and discussed. The values of the skin-friction coefficient and the local Nusselt number are given in tabular form. Copyright © 2008 John Wiley & Sons, Ltd.

Received 7 December 2007; Revised 10 March 2008; Accepted 24 March 2008

KEY WORDS: viscous fluid; heat transfer; slip flow; stretching sheet; numerical solution

1. INTRODUCTION

As evidenced by the recent literature [1–10], tremendous progress has been made in various ways for the steady flow of a stretching sheet. The work on this problem has been initiated by Sakiadis [11]. In fact, such investigations are motivated by their relevance in engineering and technology; for instance, in the aerodynamic extrusion of plastic sheets, in the boundary layer along a material handling conveyers, in the cooling of an infinite metallic plate in a cooling bath, the cooling and/or

*Correspondence to: Z. Abbas, Department of Mathematics, Faculty of Basic and Applied Sciences, IIU, Islamabad 44000, Pakistan.
†E-mail: za_qau@yahoo.com

Contract/grant sponsor: Higher Education Commission (HEC) Pakistan

drying of paper and in textile and glass fiber production. Despite such potential importance, very little work has been done on the unsteady flow induced by a stretching sheet. For a list of the basic attempts concerning with this subject, we refer the readers to the articles [12–17]. Furthermore, Wang [18] analyzed the viscous flow caused by the oscillatory stretching of a sheet.

Flow and heat transfer characteristics over a stretching sheet have important industrial applications, for instance, in the extrusion of a polymer sheet from a die. In the manufacture of such sheets, the melt issues from a slit and is subsequently stretched. The rates of stretching and cooling have a significant influence on the quality of the final product with desired characteristics. Moreover, the polymer melts often exhibit macroscopic wall slip, which in general is governed by a non-linear and monotone relationship between the slip velocity and traction. In the light of this, the purpose of this article is to study the heat transfer of a viscous fluid over an oscillatory stretching sheet with slip condition. The slip condition is taken into account in terms of the shear stress. The resulting non-linear problem is solved numerically and the influences of the various pertinent parameters are discussed.

2. FLOW ANALYSIS

Consider a two-dimensional flow of an incompressible viscous fluid over an oscillatory stretching surface at $\overline{y}=0$. Here, the $\overline{x}$-axis is taken along the stretching surface and the $\overline{y}$-axis normal to it (Figure 1). The elastic sheet is stretched back and forth with velocity $u_w=c\overline{x}\cos\omega t$ (c is the maximum stretching rate and ω is the frequency). The fluid occupies the region $\overline{y}>0$. The surface and ambient temperatures are T_w and T_∞, respectively, and $T_w>T_\infty$. In the absence of viscous dissipation, the continuity, Navier–Stokes equations and energy equations are

$$\frac{\partial u}{\partial \overline{x}}+\frac{\partial v}{\partial \overline{y}}=0 \tag{1}$$

$$\frac{\partial u}{\partial t}+u\frac{\partial u}{\partial \overline{x}}+v\frac{\partial u}{\partial \overline{y}}=-\frac{1}{\rho}\frac{\partial p}{\partial \overline{x}}+\nu\nabla^2 u \tag{2}$$

$$\frac{\partial v}{\partial t}+u\frac{\partial v}{\partial \overline{x}}+v\frac{\partial v}{\partial \overline{y}}=-\frac{1}{\rho}\frac{\partial p}{\partial \overline{y}}+\nu\nabla^2 v \tag{3}$$

$$\rho c_p\left(\frac{\partial T}{\partial t}+u\frac{\partial T}{\partial \overline{x}}+v\frac{\partial T}{\partial \overline{y}}\right)=k\nabla^2 T \tag{4}$$

where (u, v) are the velocity components in the $(\overline{x}, \overline{y})$ directions, respectively, t is the time, ν is the kinematic viscosity of fluid, ρ is the density of the fluid, p is the pressure, c_p is the specific heat at constant pressure, k is the thermal diffusivity and T is the temperature.

The corresponding slip conditions for the velocity and temperature are

$$u=u_w=c\overline{x}\cos\omega t+N\mu\frac{\partial u}{\partial \overline{y}},\quad v=0,\quad T=T_w+d\frac{\partial T}{\partial \overline{y}}\ \text{ at }\ \overline{y}=0 \tag{5}$$

$$u\to 0,\quad T\to T_\infty\ \text{ as }\ \overline{y}\to\infty \tag{6}$$

DOI: 10.1002/fld

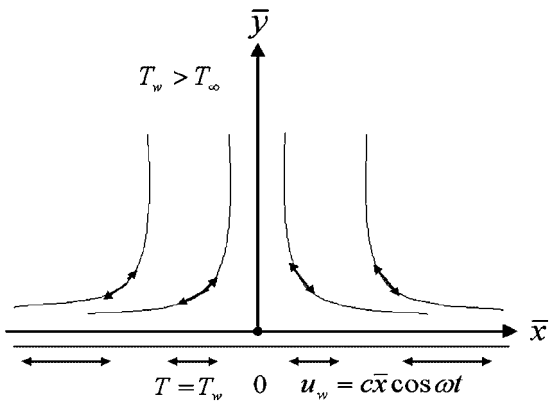

Figure 1. Geometry of the flow problem.

in which both c and ω have the dimension (time)$^{-1}$, N is a slip constant and, for $N=0$, the no-slip condition can be obtained, d is the thermal slip parameter and, for $d=0$, the thermal condition in the absence of slip can be obtained.

We define

$$S \equiv \frac{\omega}{c} \tag{7}$$

and employ the following transformations:

$$\begin{gathered} y = \sqrt{\frac{c}{v}}\bar{y}, \quad \tau = t\omega, \quad u = c\bar{x} f_y(y,\tau), \quad v = -\sqrt{vc}\, f(y,\tau) \\ \theta(y,\tau) = (T - T_\infty)/(T_\mathrm{w} - T_\infty), \quad p = p(y,\tau) \end{gathered} \tag{8}$$

then the continuity equation (1) is satisfied automatically and the governing equations (2)–(4) reduce to

$$S f_{y\tau} + f_y^2 - f f_{yy} = f_{yyy} \tag{9}$$

$$\frac{p}{\rho} = v\omega \int f_\tau \, \mathrm{d}y - \frac{v^2}{2} + v v_{\bar{y}} + \text{const} \tag{10}$$

$$\theta_{yy} + Pr(f\theta_y - S\theta_\tau) = 0 \tag{11}$$

The relevant boundary conditions (5) and (6) take the following forms:

$$f_y(0,\tau) = \cos\tau + \lambda f_{yy}(0,\tau), \quad f(0,\tau) = 0, \quad \theta(0,\tau) = 1 + \beta\theta_y(0,\tau) \tag{12}$$

$$f_y(\infty,\tau) = 0, \quad \theta(\infty,\tau) = 0 \tag{13}$$

In the above equations $Pr = \mu c_p / k$ is the Prandtl number, $\lambda = N\rho\sqrt{vc}$ is the non-dimensional slip factor and $\beta = d\sqrt{c/v}$ is the non-dimensional thermal slip parameter. Knowing the velocity field one can determine the pressure field.

DOI: 10.1002/fld

The physical quantities of interest are also the skin-friction coefficient C_f and the local Nusselt number Nu_x, which are defined as

$$C_f = \frac{\tau_w}{\rho u_w^2}, \quad Nu_x = \frac{\overline{x} q_w}{k(T_w - T_\infty)} \tag{14}$$

where τ_w and q_w are the wall skin friction and the heat transfer from the sheet, respectively. These are given by

$$\tau_w = \mu \left(\frac{\partial u}{\partial \overline{y}} \right)_{\overline{y}=0}, \quad q_w = -k \left(\frac{\partial T}{\partial \overline{y}} \right)_{\overline{y}=0} \tag{15}$$

Through the transformations (8) one obtains

$$Re_x^{1/2} C_f = f_{yy}(0, \tau), \quad Re_x^{-1/2} Nu_x = -\theta_y(0, \tau) \tag{16}$$

where $Re_x = u_w \overline{x}/\nu$ is the local Reynolds number.

3. SOLUTION OF THE PROBLEM

The coordinate transformation $\eta = 1/(y+1)$ is applied for transforming the semi-infinite physical domain $y \in [0, \infty)$ to a finite calculation domain $\eta \in [0, 1]$, i.e.

$$y = \frac{1}{\eta} - 1, \quad \frac{\partial}{\partial y} = -\eta^2 \frac{\partial}{\partial \eta}, \quad \frac{\partial^2}{\partial y^2} = \eta^4 \frac{\partial^2}{\partial \eta^2} + 2\eta^3 \frac{\partial}{\partial \eta}$$

$$\frac{\partial^2}{\partial y \partial \tau} = -\eta^2 \frac{\partial^2}{\partial \eta \partial \tau}, \quad \frac{\partial^3}{\partial y^3} = -\eta^6 \frac{\partial^3}{\partial \eta^3} - 6\eta^5 \frac{\partial^2}{\partial \eta^2} - 6\eta^4 \frac{\partial}{\partial \eta}$$

With these transformations, the differential equations (9) and (11) can be rewritten in terms of η as

$$S \frac{\partial^2 f}{\partial \tau \partial \eta} = \eta^2 \left(\frac{\partial f}{\partial \eta} \right)^2 + (6\eta^2 - 2f\eta) \frac{\partial f}{\partial \eta} + (6\eta^3 - f\eta) \frac{\partial^2 f}{\partial \eta^2} + \eta^4 \frac{\partial^3 f}{\partial \eta^3} \tag{17}$$

$$\eta^4 \frac{\partial^2 \theta}{\partial \eta^2} + 2\eta^3 \frac{\partial \theta}{\partial \eta} - Pr \left(f\eta^2 \frac{\partial \theta}{\partial \eta} + S \frac{\partial \theta}{\partial \tau} \right) = 0 \tag{18}$$

The boundary conditions (12) and (13) can be rewritten in terms of η as

$$f_\eta = 0, \quad \theta = 0 \quad \text{at } \eta = 0 \tag{19}$$

$$f = 0, \quad -\eta^2 f_\eta = \cos\tau + \lambda(\eta^4 f_{\eta\eta} + 2\eta^3 f_\eta), \quad \theta = 1 - \beta\eta^2 \theta_\eta \quad \text{at } \eta = 1 \tag{20}$$

We can discretize them for M uniformly distributed discrete points in $\boldsymbol{\eta} = (\eta_1, \eta_2, \eta_3, \ldots, \eta_{\{M\}}) \in (0, 1)$ with a space grid size of $\Delta\eta = 1/(M+1)$ and the time levels $t = (t^1, t^2, \ldots)$. Hence, the discrete values $(f_1^n, f_2^n, \ldots, f_M^n)$ and $(\theta_1^n, \theta_2^n, \ldots, \theta_M^n)$ at these grid points for the time levels $t^n = n\Delta t$ (Δt is the time step size) can be numerically solved together with the boundary conditions

DOI: 10.1002/fld

at $\eta=\eta_0=0$ and $\eta=\eta_{\{M+1\}}=1$, (19) and (20), as the initial conditions are given. We start our simulations from a motionless velocity field and a uniform temperature distribution equal to the temperature at infinity

$$f(\eta,\tau=0)=0 \quad \text{and} \quad \theta(\eta,\tau=0)=0$$

The oscillatory motion of the sheet with a temperature T_w ($\theta=1$) is suddenly set from $\tau=0$ at $\eta=1$ ($y=0$). We will see that the periodic motion will be reached after 2–4 periods. Since there are two boundary conditions for f at $\eta=1$ and only one at $\eta=0$, we cannot use central differences to approximate the third-order spatial derivative $f_{\eta\eta\eta}$ emerging in Equation (17). For the third-order derivative, the following finite-difference scheme is used, which is not central differences, and only of first-order accuracy:

$$\left.\frac{\partial^3 f}{\partial\eta^3}\right|_{\{\eta=\eta_i\}}=\frac{f_{i+2}-3f_{i+1}+3f_i-f_{i-1}}{(\Delta\eta)^3}+O(\Delta\eta^2) \tag{21}$$

where f_i is the numerical value of f at the point $\eta=\eta_i$. We construct a semi-implicit time difference for f and θ, respectively, and make sure that only linear equations for the new time step $(n+1)$ need to be solved:

$$S\frac{1}{\Delta t}\left(\frac{\partial f^{(n+1)}}{\partial\eta}-\frac{\partial f^{(n)}}{\partial\eta}\right)=\eta^2\left(\frac{\partial f^{(n)}}{\partial\eta}\right)^2+6\eta^2\frac{\partial f^{(n+1)}}{\partial\eta}-2f^{(n)}\eta\frac{\partial f^{(n)}}{\partial\eta}+6\eta^3\frac{\partial^2 f^{(n+1)}}{\partial\eta^2}$$
$$-f^{(n)}\eta^2\frac{\partial^2 f^{(n)}}{\partial\eta^2}+\eta^4\frac{\partial^3 f^{(n+1)}}{\partial\eta^3} \tag{22}$$

$$SPr\frac{(\theta^{(n+1)}-\theta^{(n)})}{\Delta t}=\eta^4\frac{\partial^2\theta^{(n+1)}}{\partial\eta^2}+2\eta^3\frac{\partial\theta^{(n+1)}}{\partial\eta}-Prf^{(n)}\eta^2\frac{\partial\theta^{(n+1)}}{\partial\eta} \tag{23}$$

It should be noted that other different choices of time differences are also possible. By means of the finite-difference method we can obtain two linear equation systems for $f_i^{(n+1)}$ and $\theta_i^{(n+1)}$ $(i=1,2,\ldots,M)$ at the time step $(n+1)$, which can be solved, e.g. by the Gaussian elimination.

4. NUMERICAL RESULTS AND DISCUSSION

We obtain the velocity and temperature fields by solving Equations (17) and (18) with boundary conditions (19) and (20) numerically for the η-coordinate. Then the numerical solutions are transformed to the physical space with y-coordinate. The velocity f' $(=f_y)$ and the temperature profile θ and the time series of the first five periods $\tau\in[0,10\pi]$ are illustrated for various values of non-dimensional relative amplitude of frequency to the stretching rate S, the slip parameter λ, the Prandtl number Pr and the thermal slip parameter β in the case of no-slip ($\lambda=0,\beta=0$) and with slip ($\lambda\neq0,\beta\neq0$). Furthermore, we compute and compare the values of skin-friction coefficient $Re_x^{1/2}C_f$ and the local Nusselt number $Re_x^{-1/2}Nu_x$ for various parameters both graphically and they are tabulated.

DOI: 10.1002/fld

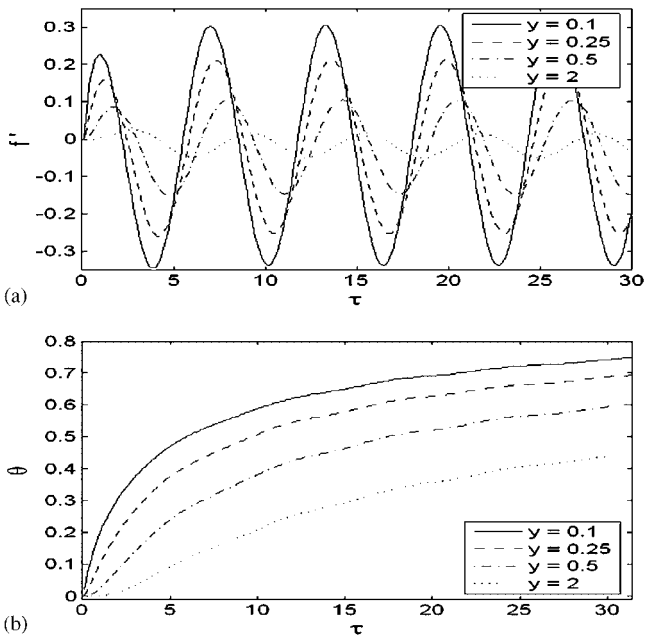

Figure 2. Time series of the flow at the four different distances from the surface for the time period $\tau \in [0, 10\pi]$: (a) the velocity field f' and (b) the temperature profile θ, with the following parameters $S = 10$, $\lambda = 0.5 = \beta$ and $Pr = 3$.

Figure 2 shows the time series of the velocity f' and the temperature field θ at four different distances from the sheet surface with fixed values of the dimensionless parameters $\lambda = 0.5$, $S = 10, Pr = 3$ and $\beta = 0.5$ for first five periods $\tau \in [0, 10\pi]$. From Figure 2(a), it can be seen that the amplitude of the flow near the oscillation surface is larger compared with that far away from the surface. With the increase in the distance from the surface, the amplitude decreases and approaches to zero. For the given motionless initial condition, a periodic motion is quickly approached, approximately 2–3 periods after the flow conditions are set. An interesting phenomenon is that a phase lag can be identified in the time series of velocity with the increases in distance from the sheet. Figure 2(b) shows that the temperature θ also decreases as the distance from the surface increases. In contrast to the time series of velocity, almost no oscillation can be identified from the time series of temperature. The temperature increases monotonically with time. It can be predicted that for $\tau \to \infty$, the dimensionless temperature θ for different distances from the sheet approaches unity, which means a uniform temperature field equal to the sheet temperature.

Figure 3 illustrates the influence of the relative amplitude of frequency to the stretching rate S on the velocity profile f' in the case of the no-slip boundary condition ($\lambda = 0$) for four different times $\tau = 8.5\pi, 9\pi, 9.5\pi$ and 10π in the fifth period for which a periodic motion has been reached. The transverse profiles of velocity are illustrated only for the boundary layer near the sheet, $y \in [0, 10]$, above which the velocity is negligible. Figure 3(a) shows that at $\tau = 8.5\pi$, the velocity f' is zero at the surface $y = 0$ due to the no-slip condition and far away from the sheet it approaches to zero again. It can also be seen that initially the velocity f' increases with the increase in the distance near the sheet, then it decreases and oscillates becoming negative. This again shows the phase lag

DOI: 10.1002/fld

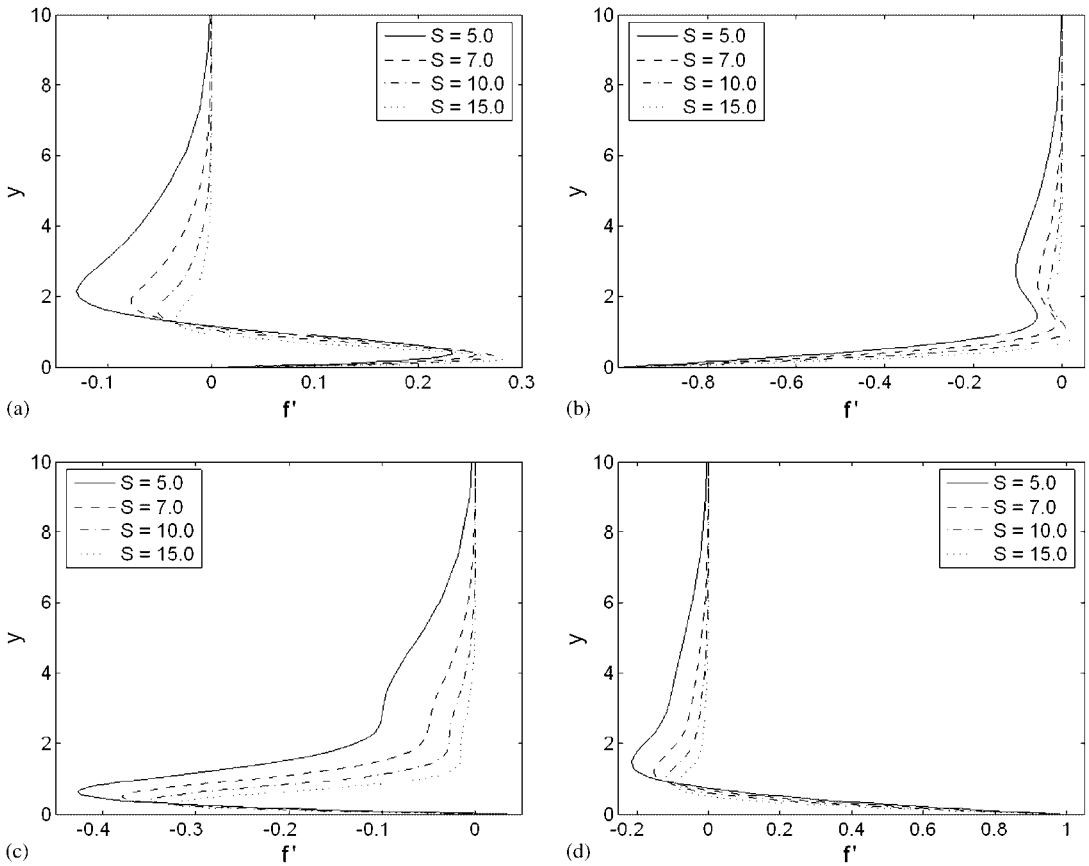

Figure 3. Transverse profiles of the velocity field f' at the four different values of S for the fifth period $\tau \in [8\pi, 10\pi]$ for which a periodic velocity field has been reached: (a) $\tau = 8.5\pi$; (b) $\tau = 9\pi$; (c) $\tau = 9.5\pi$; and (d) $\tau = 10\pi$ in the case of no-slip $\lambda = 0$.

between the flow and the oscillation of the sheet. It indicates that along the transverse direction a phase difference larger than π may occur. The velocity profiles for several other time points within the fifth period are displayed in Figures 3(b)–(d). It can also be seen that the velocity field is not in phase with the sheet oscillation. With the increase in the distance from the sheet, the phase displacement increases. Furthermore, when S increases, the oscillation amplitude of the velocity decreases.

Figure 4 is plotted for the variations of the slip parameter λ on the velocity profile f' by keeping $S = 10$ fixed for the different times of $\tau \in [8.5\pi, 9\pi, 9.5\pi, 10\pi]$ in the fifth period, respectively. When slip occurs ($\lambda \neq 0$), the flow velocity near the sheet is no longer equal to the sheet oscillation velocity, i.e. a velocity slip exists. With the increase in λ, such a slip velocity increases. Furthermore, increasing the value of λ will decrease the flow velocity amplitude, because under the slip condition the propulsion of the oscillatory sheet can be only partly transmitted to the fluid.

Figure 5 elucidates the effects of the relative amplitude of frequency to the stretching rate S (panels a and b) and the slip parameter λ (panel c) on the time series of velocity at a fixed

DOI: 10.1002/fld

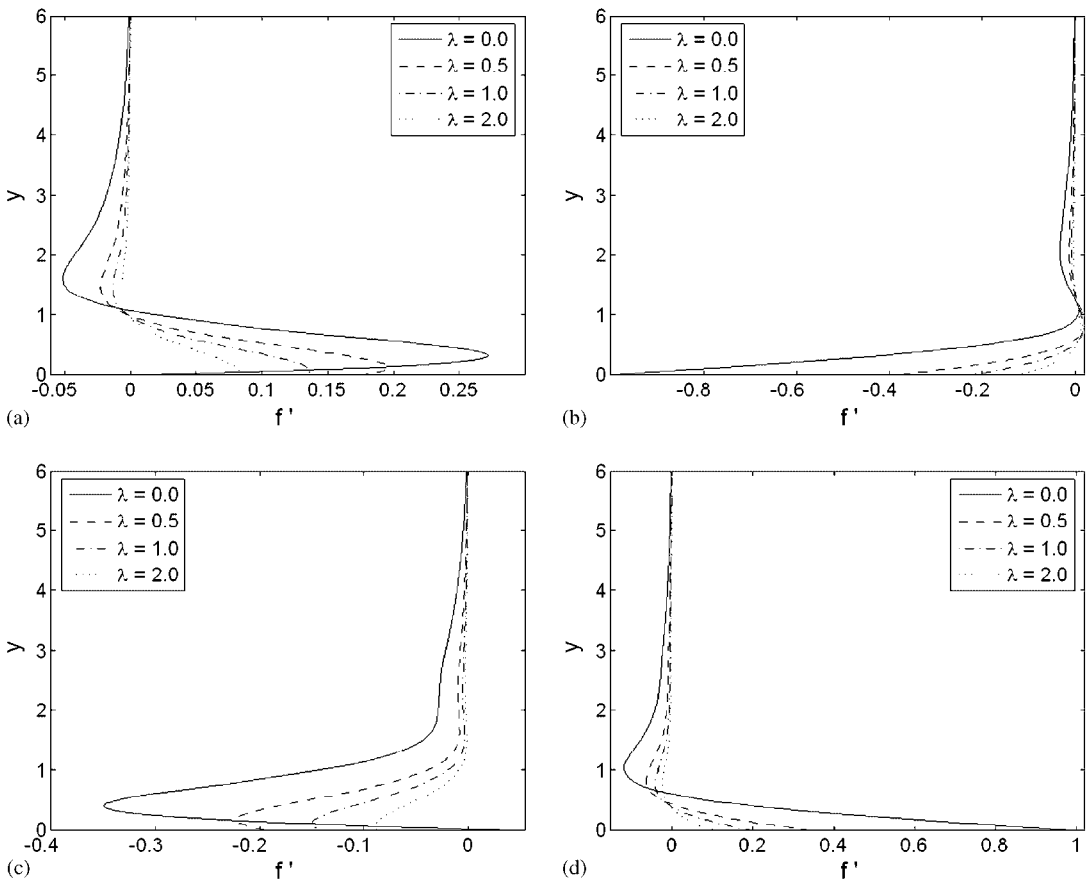

Figure 4. Transverse profiles of the velocity field f' at the four different values of λ for the fifth period $\tau \in [8\pi, 10\pi]$ for which a periodic velocity field has been reached: (a) $\tau = 8.5\pi$; (b) $\tau = 9\pi$; (c) $\tau = 9.5\pi$; and (d) $\tau = 10\pi$ with $S = 10$ in the case of slip condition at the sheet (surface).

distance ($y = 0.25$) from the sheet for the first five periods $\tau \in [0, 10\pi]$ in the case of no-slip ($\lambda = 0$ in panel (a)) and with slip ($\lambda = 0.5$ in panel (b)). The amplitude of the flow velocity decreases as S increases. With the increase in S, a slightly increasing phase shift can be identified. For a slip condition ($\lambda = 0.5$ in Figure 5(b)), the velocity amplitude decreases substantially. Figure 5(c) shows the influence of the slip parameter λ with fixed $S = 10$. The amplitude of the external flow decreases monotonically with the increase in λ.

Figure 6 is plotted to see the effects of four different time points τ within the fifth period (corresponding to the periodic motion) on the velocity f' with fixed slip parameter $\lambda = 0.5$ and $S = 10$. The oscillations of the velocity profiles, the phase lag and the attenuation of the velocity with the distance from the plate can be clearly observed again.

Figures 7–9 show the influence of the relative amplitude of frequency to the stretching rate S, the Prandtl number Pr and the thermal slip parameter β on the temperature field θ. Figure 7 gives the effects of the varying S and Pr on the temperature profiles $\theta(y)$ in case of no-thermal slip

DOI: 10.1002/fld

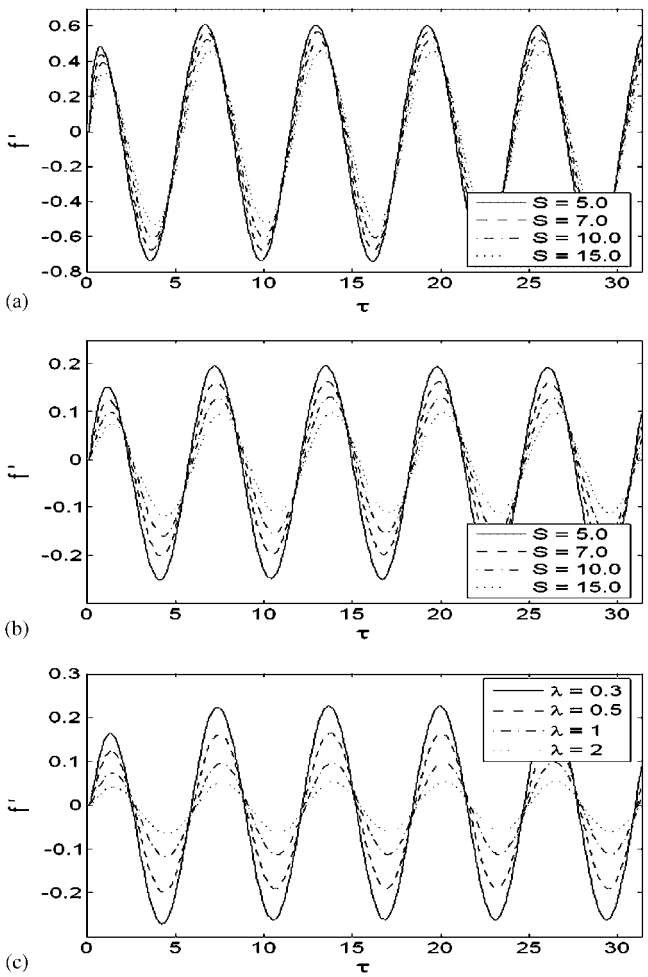

Figure 5. Time series of the velocity field f' in the first five periods $\tau \in [0, 10\pi]$ at a fixed distance to the sheet, $y = 0.25$: (a) effects of S with the no-slip condition at the sheet (surface) $\lambda = 0$; (b) effects of S with the slip condition at the sheet (surface) $\lambda = 0.5$; and (c) effects of slip parameter λ for the fixed value of $S = 15$.

($\beta = 0$) in the fixed time $\tau = 8\pi$. It is observed from Figure 7(a) that the temperature is a decreasing function of S. It means that increasing S prevents and slows down the heat transfer from the sheet. As expected, Figure 7(b) shows that the temperature decreases for the large values of the Prandtl number Pr due to the decreased thermal diffusivity.

Figure 8(a) gives the variations of the thermal slip parameter β on the temperature profile at the time $\tau = 8\pi$ by keeping $S = 15$ and $Pr = 5$ fixed. As the thermal slip parameter β increases, less heat is transferred from the sheet to the fluid; hence, the temperature values θ for all distances decreases. Figure 8(b) illustrates the temperature profiles for four different times τ with $\beta = 0.5$, $S = 10$ and $Pr = 2$. As expected, as the time increases, more heat is transferred to the fluid and θ increases.

DOI: 10.1002/fld

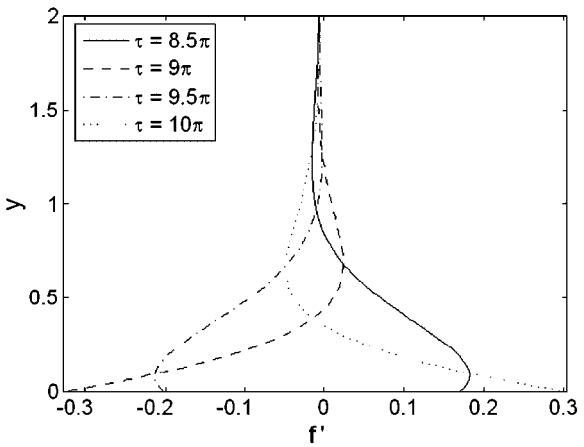

Figure 6. Transverse profiles of the velocity field f' at the four different time points of τ in the fifth period with $\lambda=0.5$ and $S=15$.

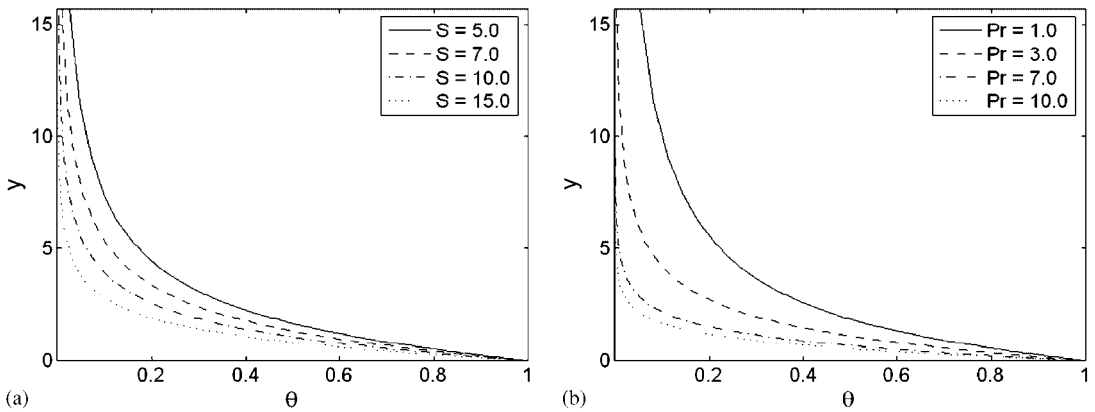

Figure 7. Transverse profile of the temperature θ at $\tau=8\pi$ in the case of no-thermal slip $\beta=0$: (a) for various values of S with $Pr=5$ and $\lambda=0.5$ and (b) for various values of the Prandtl number Pr with $S=15$ and $\lambda=0.5$.

Figure 9 depicts the results of varying S, Pr and β, respectively, on the time series of the temperature θ. As shown in the transverse profiles of temperature θ for different values of S for a fixed time (Figure 7(a)), similar results can also be seen for the corresponding time series. Figure 9(a) shows the change of the temperature with respect to S for no-thermal slip ($\beta=0$). It can be seen that with the increase in S, i.e. with the increase in the sheet oscillatory frequency or the decrease in the oscillatory amplitude the increase in the temperature θ with time becomes slower. Furthermore, a small oscillation, which is superimposed on the monotonically increasing temperature time series, can be identified for small values of S. Similarly, with the increase in Pr, i.e. the increase in the specific heat or the decrease in the thermal diffusivity, the increase

DOI: 10.1002/fld

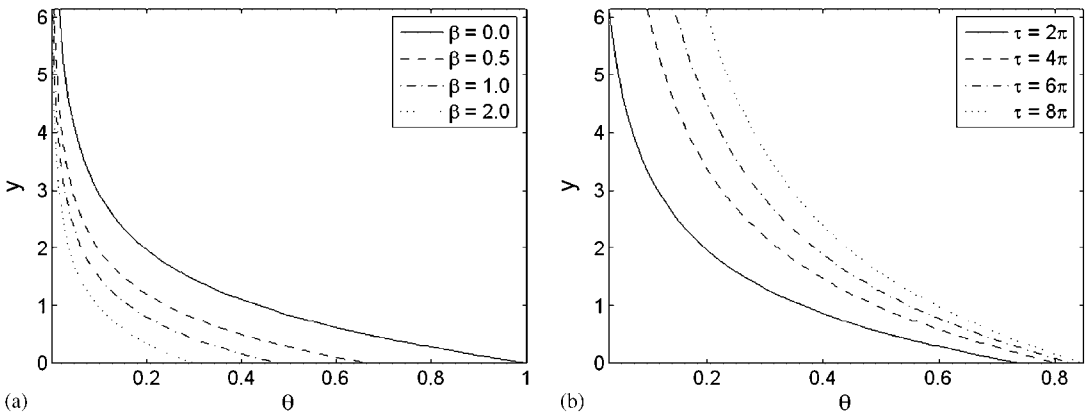

Figure 8. The transverse profiles of the temperature θ: (a) for various values of the thermal slip parameter β as well as $\tau=8\pi$, $Pr=5$, $S=15$, $\lambda=0.5$ and (b) for the four different times as well as $\beta=0.5$, $S=10$, $Pr=1$ and $\lambda=0.5$.

in the fluid temperature becomes slower, as shown in Figure 9(b). Figure 9(c) shows that for a slip thermal condition at the sheet much less heat is transferred to the fluid, the fluid temperature increases much slower than that with a no-slip thermal condition.

Figures 10 and 11 show the influence of the relative amplitude of frequency S, the flow slip parameter λ, the Prandtl number Pr and the thermal slip parameter β on the skin-friction coefficient $Re_x^{1/2}C_f$ and the local Nusselt number $Re_x^{-1/2}Nu_x$. Figure 10(a) elucidates the effects of S on the skin-friction coefficient $Re_x^{1/2}C_f$ at fixed value of $\lambda=1$. It is observed that due to the oscillatory motion of the sheet, the skin-friction coefficient $Re_x^{1/2}C_f$ also varies periodically and its amplitude increases with an increase in S. It means that with the increase in S, less momentum is transmitted from the oscillating sheet to the fluid. Figure 10(b) gives the variations of the slip parameter λ on the skin-friction coefficient $Re_x^{1/2}C_f$ at fixed $S=15$. As expected the oscillatory amplitude of the skin-friction coefficient $Re_x^{1/2}C_f$ decreases as the value of λ increases, i.e. the slip condition reduces the momentum transfer from the sheet to the fluid.

Figure 11 shows the physical significance of S, Pr and β on the local Nusselt number $Re_x^{-1/2}Nu_x$. Figure 11(a) illustrates the effects of S on the local Nusselt number $Re_x^{-1/2}Nu_x$ with fixed $Pr=3$, $\beta=0.3$ and $\lambda=1$. It is noted that for $\tau=0$, the local Nusselt number $Re_x^{-1/2}Nu_x$ has its maximum and then decreases monotonically because for the given initial conditions the temperature gradient at the sheet surface has its maximum initially and decreases with time. The local Nusselt number $Re_x^{-1/2}Nu_x$ increases with the increase in S. A slight oscillation can be identified from the time series with $S=5$. We can see from Figure 11(b) that the magnitude of the local Nusselt number $Re_x^{-1/2}Nu_x$ is also increased as Pr increases. The variation of the thermal slip parameter β on the local Nusselt number $Re_x^{-1/2}Nu_x$ can be seen from Figure 11(c). It is observed that the local Nusselt number $Re_x^{-1/2}Nu_x$ has opposite effects for the values of β in contrast with the case of S and Pr. The magnitude of the local Nusselt number decreases as the thermal slip parameter increases. To sum up, increasing S and Pr will increase the heat transfer from the sheet to the fluid, while increasing β will reduce this effect.

DOI: 10.1002/fld

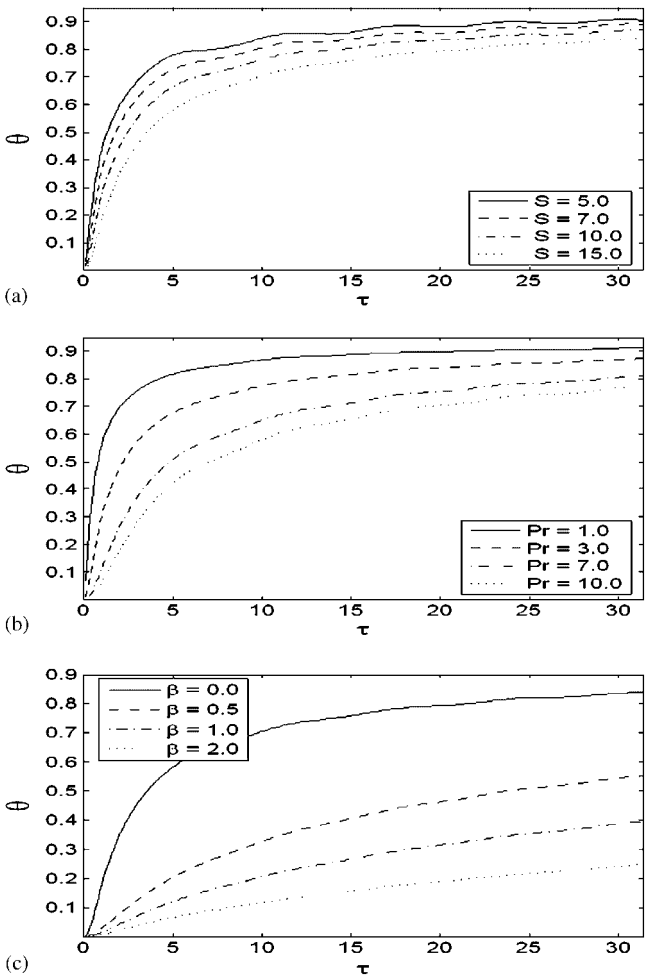

Figure 9. Time series of the temperature θ in the first five periods $\tau \in [0, 10\pi]$ at $y = 0.25$: (a) effects of S with no-thermal slip at the sheet (surface) $\beta = 0$; (b) effects of Pr with no-thermal slip at the sheet (surface) $\beta = 0$; and (c) effects of thermal slip parameter β with $S = 15$ and $Pr = 3$.

Tables I and II quantitatively show the values of the skin-friction coefficient $Re_x^{1/2} C_f$ and the local Nusselt number $Re_x^{-1/2} Nu_x$ for the different values of relative amplitude of frequency to stretching rate S, the slip parameter λ, the thermal slip parameter β and the Prandtl number Pr. Table I shows the values of the skin-friction coefficient $Re_x^{1/2} C_f$ and the local Nusselt number $Re_x^{-1/2} Nu_x$ for the various values of S and λ at the time periods $\tau = 2\pi$ and 8π, respectively. It is noted that the magnitude of the skin-friction coefficient $Re_x^{1/2} C_f$ increases as the values of S are increased for both time periods $\tau = 2\pi$ and 8π. The increment in the values of skin-friction coefficient is larger at the time period $\tau = 8\pi$ when compared with the time period $\tau = 2\pi$. The local Nusselt number $Re_x^{-1/2} Nu_x$ is also increased as S increases for the both time periods $\tau = 2\pi$

DOI: 10.1002/fld

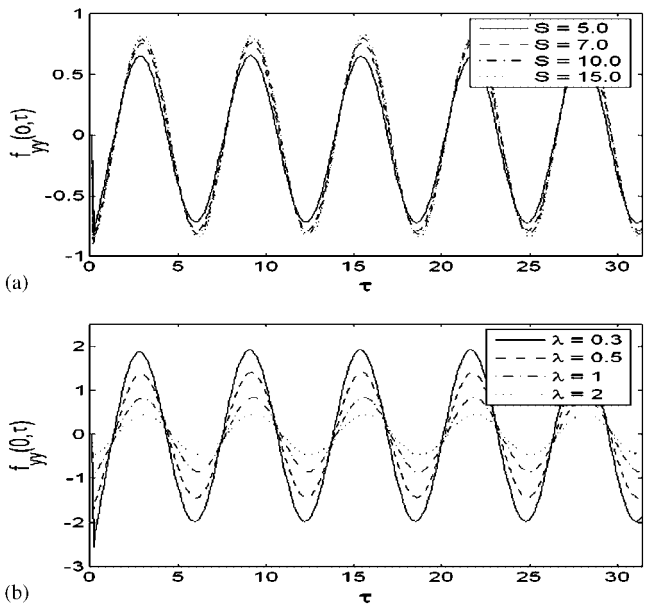

Figure 10. Time series of the skin-friction coefficient $Re_x^{1/2}C_f$ in the first five periods $\tau \in [0, 10\pi]$: (a) effects of S with slip at the sheet (surface) $\lambda = 1$ and (b) effects of the slip parameter λ with $S = 15$.

and 8π, but this change in the local Nusselt number is larger at the period $\tau = 2\pi$. The magnitudes of the skin-friction coefficient $Re_x^{1/2}C_f$ are decreased considerably, while the values of the local Nusselt number $Re_x^{-1/2}Nu_x$ are increased only slightly for large values of the slip parameter λ at both time periods $\tau = 2\pi$ and 8π. Table II gives the values of the local Nusselt number $Re_x^{-1/2}Nu_x$ for different values of the thermal slip parameter β, the Prandtl number Pr and the four different time periods $\tau = 2\pi, 4\pi, 6\pi, 8\pi$. It can be seen that the local Nusselt number $Re_x^{-1/2}Nu_x$ decreases as the values of the thermal slip parameter β increase for all four time periods $\tau = 2\pi, 4\pi, 6\pi, 8\pi$ and values of the local Nusselt number are also decreased when the time periods increase due to the decrease in the temperature gradient near the sheet. This table also shows that the local Nusselt number $Re_x^{-1/2}Nu_x$ increases for the large values of Prandtl number Pr.

5. CONCLUSIONS

In this paper we investigated the flow and heat transfer problem of a viscous fluid in a semi-infinite space due to the oscillation of an infinite stretching and warmer surface with/without flow/thermal slip conditions. A coordinate transformation is employed to transform the semi-infinite flow domain to a finite computational domain and a suitable finite-difference method is used to solve the governing partial differential equations. The time series of the flow velocity, the temperature, the structure of the boundary layer near the sheet, the influences of the different values of the relative amplitude of frequency to stretching rate S, the Prandtl number Pr and, especially, the flow slip

DOI: 10.1002/fld

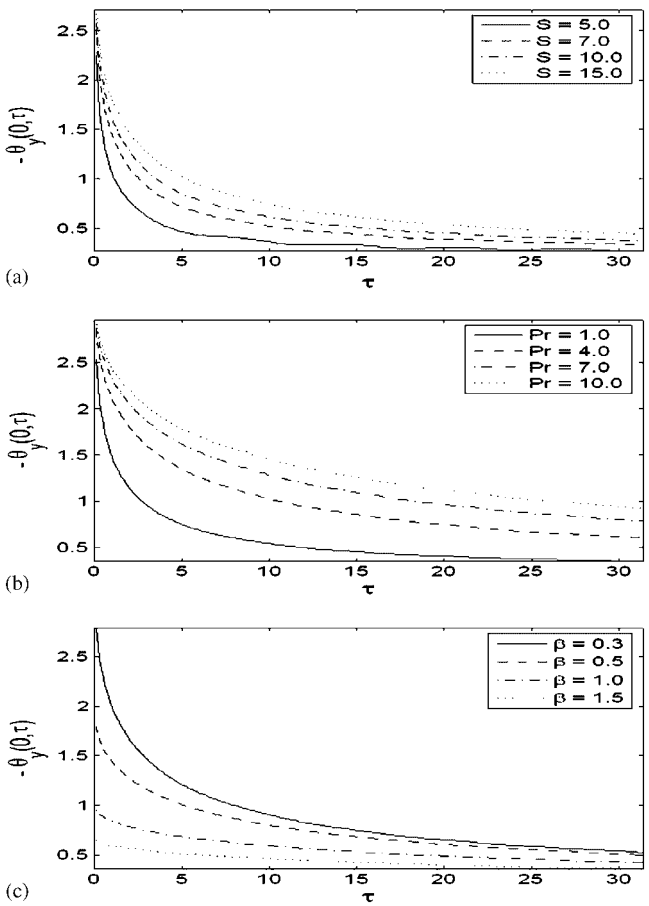

Figure 11. Time series of he local Nusselt number $Re_x^{-1/2}Nu_x$ in the first five periods $\tau \in [0, 10\pi]$: (a) effects of S with no-thermal slip at the sheet (surface) $\beta = 0$ and $Pr = 2$; (b) effects of Prandtl number Pr with no-thermal slip at the sheet (surface) $\beta = 0$ and $S = 15$; and (c) effects of the thermal slip parameter β with $S = 15$, $Pr = 5$ and $\lambda = 0.5$.

parameter λ and the thermal slip parameter β at the sheet are graphically presented and discussed. The following conclusions may be extracted from the numerical results:

- When a periodically oscillating sheet is suddenly put into the viscous fluid, a periodic motion can rapidly be observed, at most after three or four periods.
- The oscillation of the temperature time series can hardly be identified; the fluid temperature increases with time monotonically.
- There exists a phase lag between the flow velocity and the sheet oscillation, which increases with the distance from the sheet, up to a phase difference larger than π.
- The flow exists only within a shear layer near the sheet, while the heat can transfer to an infinitely large distance with the increase in time.

DOI: 10.1002/fld

Table I. The values of the skin-friction coefficient $Re_x^{1/2}C_f$ and the local Nusselt number $Re_x^{-1/2}Nu_x$ for different values of S, λ and two different time points when $\beta=0.5$ and $Pr=1$.

		$\tau=2\pi$		$\tau=8\pi$	
S	λ	$Re_x^{1/2}C_f$	$Re_x^{-1/2}Nu_x$	$Re_x^{1/2}C_f$	$Re_x^{-1/2}Nu_x$
3	0.5	−0.991348	0.326176	−1.038528	0.257534
5	0.5	−1.110076	0.390433	−1.136707	0.277388
10	0.5	−1.288023	0.521208	−1.303137	0.317028
15	0.5	−1.387906	0.620067	−1.398357	0.356688
20	0.5	−1.453961	0.698117	−1.461767	0.394677
10	0.0	−2.478828	0.520770	−2.591060	0.314812
10	0.5	−1.288023	0.521208	−1.303137	0.317028
10	1.0	−0.800192	0.522412	−0.804338	0.318404
10	2.0	−0.447958	0.523418	−0.448734	0.319411
10	3.0	−0.309987	0.523835	−0.310217	0.319794
10	5.0	−0.191544	0.524201	−0.191563	0.320115

Table II. The values the local Nusselt number $Re_x^{-1/2}Nu_x$ for different values of β, Pr and four different time points when $S=10$ and $\lambda=0.5$.

		$\tau=2\pi$	$\tau=4\pi$	$\tau=6\pi$	$\tau=8\pi$
β	Pr	$Re_x^{-1/2}Nu_x$	$Re_x^{-1/2}Nu_x$	$Re_x^{-1/2}Nu_x$	$Re_x^{-1/2}Nu_x$
0.0	1.0	0.567704	0.429927	0.380987	0.356762
0.3	1.0	0.550257	0.409161	0.357609	0.331728
0.5	1.0	0.521208	0.392740	0.342794	0.317028
1.0	1.0	0.436805	0.346426	0.305842	0.283197
2.0	1.0	0.312979	0.267130	0.243003	0.228041
3.0	1.0	0.240492	0.213634	0.198383	0.188377
5.0	1.0	0.163227	0.150957	0.143468	0.138273
7.0	1.0	0.123270	0.116301	0.111899	0.108761
0.5	0.0	0.275358	0.275358	0.275358	0.275358
0.5	0.5	0.394987	0.318701	0.294697	0.284209
0.5	1.0	0.521208	0.392740	0.342794	0.317028
0.5	3.0	0.810907	0.615329	0.518054	0.457851
0.5	5.0	0.963344	0.755444	0.642523	0.567944
0.5	7.0	1.063076	0.854542	0.735532	0.653956
0.5	10.0	1.165156	0.961632	0.840072	0.753805
0.5	50.0	1.538309	1.397107	1.300617	1.224600
0.5	100.0	1.648709	1.538027	1.459846	1.396667

- Increasing the flow slip parameter causes the decrease in the amplitude of the flow velocity, while with the increase in the thermal slip parameter the heat transfer from the sheet to the fluid becomes slower.
- Increasing the relative amplitude of frequency to stretching rate S causes the decrease in the velocity amplitude and diminishes the heat transfer.
- With the increase in the Prandtl number, the heat transfer from the sheet to fluid becomes slower.

DOI: 10.1002/fld

ACKNOWLEDGEMENTS

We are grateful to the reviewers for the useful suggestions. One of the authors Z. Abbas gratefully acknowledges the support provided for this study by the Higher Education Commission (HEC) Pakistan under the International Research Support Initiative Program (IRSIP).

REFERENCES

1. Sajid M, Hayat T. Non-similar series solution for boundary layer flow of a third order fluid over a stretching sheet. *Applied Mathematics and Computation* 2007; **189**:1576–1585.
2. Ariel PD, Hayat T, Asghar S. Homotopy perturbation method and axisymmetric flow over a stretching sheet. *International Journal of Nonlinear Science and Numerical Simulation* 2006; **7**:399–406.
3. Hayat T, Sajid M. Analytic solution for axisymmetric flow and heat transfer of a second grade fluid past a stretching sheet. *International Journal of Heat and Mass Transfer* 2007; **50**:75–84.
4. Sajid M, Hayat T, Asghar S. Non-similar solution for the axisymmetric flow of a third grade fluid over a radially stretching sheet. *Acta Mechanica* 2007; **189**:193–205.
5. Wang CY. Flow due to a stretching boundary with partial slip-an exact solution of the Navier–Stokes equations. *Chemical Engineering Science* 2002; **57**:3745–3747.
6. Cortell R. A note on magnetohydrodynamic flow of a power-law fluid over a stretching sheet. *Applied Mathematics and Computation* 2005; **168**:557–566.
7. Cortell R. A note on flow and heat transfer of a viscoelastic fluid over a stretching sheet. *International Journal of Non-linear Mechanics* 2006; **41**:78–85.
8. Vajravelu K, Rollins D. Hydromagnetic flow of second grade fluid over a stretching sheet. *Applied Mathematics and Computation* 2004; **148**:783–791.
9. Liu IC. Flow and heat transverse of an electrically conducting fluid of second grade over a stretching sheet subject to a transverse magnetic field. *International Journal of Heat and Mass Transfer* 2004; **47**:4427–4437.
10. Hayat T, Abbas Z, Sajid M. Series solution for the upper convected Maxwell fluid over a porous stretching plate. *Physics Letters A* 2006; **358**:396–403.
11. Sakiadis BC. Boundary-layer behavior on continuous solid surfaces: II. The boundary layer on a continuous flat surface. *AIChE Journal* 1961; **7**:221–227.
12. Pop I, Na TY. Unsteady flow past a stretching sheet. *Mechanics Research Communications* 1996; **23**:413–422.
13. Nazar R, Amin N, Pop I. Unsteady boundary layer flow due to a stretching surface in a rotating fluid. *Mechanics Research Communications* 2004; **31**:121–128.
14. Liao SJ. An analytic solution of unsteady boundary layer flows caused by an impulsively stretching plate. *Communications in Nonlinear Science and Numerical Simulation* 2006; **11**:326–339.
15. Wang C, Pop I. Analysis of the flow of a power-law fluid film on an unsteady stretching surface by means of homotopy analysis method. *Journal of Non-Newtonian Fluid Mechanics* 2006; **138**:161–172.
16. Xu H, Liao SJ. Series solution of unsteady magnetohydrodynamic flows of non-Newtonian fluids caused by an impulsively stretching plate. *Journal of Non-Newtonian Fluid Mechanics* 2005; **129**:46–55.
17. Sajid M, Ahmad I, Hayat T, Ayub M. Series solution for unsteady axisymmetric flow and heat transfer over a radially stretching sheet. *Communications in Nonlinear Science and Numerical Simulation*, in press.
18. Wang CY. Nonlinear streaming due to the oscillatory stretching of a sheet in a viscous fluid. *Acta Mechanica* 1988; **72**:261–268.

DOI: 10.1002/fld